

Communication

Adaptive Terminal Sliding Mode Control of Picking Manipulator Based on Uncertainty Estimation

Caizhang Wu and Shijie Zhang * 

College of Electrical Engineering, Henan University of Technology, Zhengzhou 450001, China

* Correspondence: zhangshijie@haut.edu.cn; Tel.: +86-18-6237-18217

Abstract: In this paper, a robust nonsingular fast terminal sliding mode control scheme for the picking manipulator under the condition of load change and nonlinear friction disturbance is presented. Firstly, the dynamic equation of the picking manipulator under the condition of load change and nonlinear friction disturbance is established. Then, in order to avoid the singularity problem existing in the terminal sliding mode and improve the convergence time, a new nonsingular fast terminal sliding mode control strategy is adopted to design the control law of the picking manipulator, which can guarantee the finite time convergence. The adaptive law is used to estimate the uncertainties of the system, and the finite time convergence of the system state is proved by the Lyapunov criterion. In addition, the genetic algorithm is used to identify the friction parameters to realize the nonlinear friction compensation control of the system. Finally, the simulation results of the picking manipulator under different load conditions show that the controller designed in this paper realizes the fast and accurate positioning of the picking manipulator under load change and nonlinear friction, and the control strategy is reasonable and effective.

Keywords: picking manipulator; sliding mode control; adaptive control; friction compensation; genetic algorithm



Citation: Wu, C.; Zhang, S. Adaptive Terminal Sliding Mode Control of Picking Manipulator Based on Uncertainty Estimation. *Actuators* **2022**, *11*, 347. <https://doi.org/10.3390/act11120347>

Academic Editors: Marco Carricato and Edoardo Ida

Received: 21 October 2022

Accepted: 18 November 2022

Published: 25 November 2022

Publisher's Note: MDPI stays neutral with regard to jurisdictional claims in published maps and institutional affiliations.



Copyright: © 2022 by the authors. Licensee MDPI, Basel, Switzerland. This article is an open access article distributed under the terms and conditions of the Creative Commons Attribution (CC BY) license (<https://creativecommons.org/licenses/by/4.0/>).

1. Introduction

An agricultural picking manipulator is a kind of mechatronics system with variable parameters and strong nonlinearity [1,2]. Under the action of nonlinear uncertain factors such as the weight change of the picking object and friction disturbance, the general proportional integral derivative (PID) controller does not enable the picking manipulator to obtain reliable control performance, so the mechanical holding brake has to be used for positioning in engineering [3,4]. However, this mechanical positioning method will cause greater impact wear, reduce the service life of the picking manipulator, and seriously reduce its overall performance. Therefore, how to design a robust controller for the picking manipulator is an urgent problem to be solved.

The sliding mode control is one of the control methods to deal with nonlinear systems with parameter perturbation and external disturbance [5–7]. This method has the advantages of strong robustness and easy design, so it has been widely used in a variety of fields [8–11]. With the sliding mode control of the linear switching function, the error between the system state and the expected state converges exponentially, and the system state can only approach the expected trajectory, but cannot reach the expected trajectory. Therefore, Refs. [12–14] proposed the terminal sliding mode (TSM) control. By introducing a nonlinear term into the construction of the sliding mode switching function, the tracking error on the sliding mode surface can converge to zero in a finite time, which solves the problem that the traditional sliding mode control can only converge asymptotically under the action of the linear sliding mode surface. However, the control effect of terminal sliding mode control in a singular control region will tend to infinity, which is not conducive to practical application.

The nonsingular terminal sliding mode (NTSM) control strategy is designed in [15–18], which avoids the singular problem of control when constructing the sliding mode switching function, retains the finite time convergence characteristics, and can obtain higher convergence accuracy. Because the NTSM control method has good control performance, it has been widely used. The authors in [19] combine the advantages of the linear sliding mode and NTSM. The hybrid NTSM control is designed to make the convergence of the system faster. Compared with the proportional-integral (PI) controller, it enhances the robustness of the permanent magnet synchronous motor.

Compared with the linear sliding mode, the NTSM has a higher convergence speed when the system state is close to the equilibrium point, but when the system state is far from the equilibrium point, its convergence time is longer and the dynamic characteristics become worse. In order to avoid the control singularity problem and accelerate the convergence speed when the system is far from the sliding mode surface, in this paper, a new nonsingular fast terminal sliding mode (NFTSM) control strategy is used to design the control law. In the actual process of realizing the sliding mode control, how to determine the switching gain of the sliding mode control is a difficult problem. Usually, the upper bound of the uncertainty in the system is unknown. In order to ensure the good robustness of the control system, the switching gain needs to be large enough [20]. However, excessive switching gain will cause control chattering. In order to reduce system chattering, this paper uses an adaptive control strategy to estimate the uncertain upper bound of the system, so there is no need to know the prior knowledge of the uncertain upper bound, which is conducive to practical application.

Recently, a robust sliding mode-based learning control strategy for a class of nonlinear discrete-time descriptor systems with time-varying delay and external disturbance was developed in [21]. The authors in [22] discussed the control problem of nonlinear disturbed polynomial systems using the formalism of output feedback linearization and a subsequent sliding mode control design. The authors in [23] proposed a novel developed a photovoltaic model based on an improved arithmetic optimization algorithm to extract the solar cell parameters. A neuroadaptive learning algorithm for constrained nonlinear systems with disturbance rejection is proposed in [24,25].

In this paper, an adaptive non-singular fast terminal sliding mode (ANFTSM) control method for the picking manipulator is used to design the corresponding position controller, which avoids the singularity problem of the traditional terminal sliding mode control and the slow convergence of the traditional NTSM control. At the same time, the adaptive estimation of the system uncertainty is used without the prior knowledge of the upper bound of the uncertainty, which effectively reduces the chattering caused by the excessive switching gain. Meanwhile, the genetic algorithm is used to identify the parameters of the nonlinear friction torque in the motion process of the picking manipulator, and the corresponding compensation control is designed. The main contributions of this paper are highlighted as follows. (1) The disturbance existing in the manipulator system is estimated adaptively, and the estimated value is used as a feedback signal to provide compensation for the controller, so as to improve the tracking performance of the system and enhance the robustness of the system. (2) A nonsingular fast terminal sliding surface is constructed to solve the singularity problem of the controller and obtain a finite time stability result, ensuring the convergence speed and transient response performance of the system control. (3) A nonsingular fast terminal sliding mode controller based on friction compensation is constructed. By introducing a saturation function instead of a symbolic function, the chattering problem is further weakened and the desired tracking trajectory of each joint is tracked quickly and accurately.

This paper is divided into five sections. The next section introduces the dynamic model of the picking manipulator and the description of the problem to be solved in this paper. The ANFTSM controller design method and stability analysis for the picking manipulator are proposed in Section 3. According to the controller designed in Section 3,

the corresponding simulation results are given in Section 4, followed by a brief conclusion in Section 5.

2. Preliminaries

2.1. Dynamic Model of Picking Manipulator

The structure of the picking manipulator is shown in Figure 1. The DC motor drives the manipulator arm to rotate around the trunnion through the reducer, and the equilibrator is used to balance the load torque to reduce the working load of the driving motor.

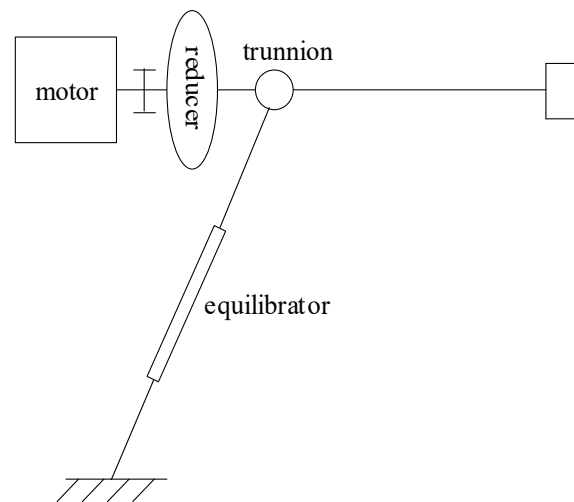


Figure 1. The structural diagram of the picking manipulator.

The picking manipulator is regarded as a single-degree-of-freedom manipulator, and its dynamic equation is [26]

$$J\ddot{\theta} = T \quad (1)$$

where J is the equivalent rotational inertia of the system. θ and $\ddot{\theta}$ are the rotation angle and angular acceleration of the picking manipulator, respectively. T is the equivalent rotation torque acting on the manipulator.

$$T = i_1 \eta_1 k_T I - T_R + T_G - T_f + D \quad (2)$$

where i_1 is the total transmission ratio of the system, η_1 is the transmission efficiency of the reducer, k_T is the motor torque constant, I is the control current of the motor, T_R is the torque of the equilibrator to the manipulator, and T_G is the gravity torque of the manipulator, which depends on the rotation angle of the manipulator. T_f is the friction torque to be identified, and D is an uncertainty term caused by parameter changes, unmodeled dynamics, and external disturbances.

The equilibrator is composed of an oil cylinder and accumulator, in which the oil cylinder pressure is

$$p = p_0 S \left(\frac{V_0}{V_0 - \Delta V} \right)^n \quad (3)$$

where p_0 is the initial pressure of the accumulator, S is the piston area of the cylinder, V_0 is the initial volume of gas, ΔV is the volume of gas change, and n is the polytropic index of the gas. Then, the torque of the equilibrator to the manipulator can be written as

$$T_R = l p_0 S \left(\frac{V_0}{V_0 - \Delta L S} \right)^n \quad (4)$$

where l is the distance from the center of rotation to the balancer, and ΔL is the distance of the piston movement.

2.2. Problem Description

Design an adaptive non-singular fast terminal sliding mode (ANFTSM) controller for the above picking manipulator to ensure that the joint position of the picking manipulator tracks the desired trajectory, and the tracking error can converge to a neighborhood near zero in a finite time.

3. Controller Design of the Picking Manipulator

3.1. ANFTSM Controller

By defining $\theta = x_1, \ddot{\theta} = x_2$, the dynamic equation of the picking manipulator can be simplified into the following second-order nonlinear uncertain system.

$$\begin{cases} \dot{x}_1 = x_2 \\ \dot{x}_2 = \frac{k_T i_1 \eta_1}{J} u + \frac{1}{J} (T_G - T_R - T_f) + d \\ y = x_1 \end{cases} \quad (5)$$

where $d = D/J$ is an uncertainty term, and $|d| \leq U$, U is a constant. u is the control input, and y is the system output. The following assumptions are assumed to be fulfilled henceforth.

Assumption 1: The states of the picking manipulator system are uniformly bounded.

Assumption 2: The uncertainty of the system is continuously differentiable and bounded at all times.

The angular displacement error of the picking manipulator is defined as

$$\begin{cases} e = x_1 - x_d \\ \dot{e} = \dot{x}_1 - \dot{x}_d \\ \ddot{e} = \ddot{x}_1 - \ddot{x}_d \end{cases}$$

where x_d is a given expected value.

For equation (5), the traditional TSM switching function is generally designed as

$$s = \dot{e} + \alpha e^{q/p} \quad (6)$$

where s is sliding mode switching function, $\alpha > 0$ is a constant, p and q are positive odd number, and $p > q$.

Then, the traditional TSM controller is designed as

$$u = \frac{J}{k_T i_1 \eta_1} (\ddot{x}_d - \frac{1}{J} (T_G - T_R - T_f) - \alpha \frac{q}{p} e^{q/p-1} \dot{e} - (U + \eta) \text{sgn}(s)) \quad (7)$$

where $\eta > 0$ is the design constant, $\text{sgn}(\cdot)$ is a symbol function.

It can be seen from (7) that the control quantity contains a $\alpha \frac{q}{p} e^{q/p-1} \dot{e}$ term, which contains a negative exponential term, that is, the index $q/p - 1 < 0$. Therefore, when $e = 0, \dot{e} \neq 0$, the control quantity tends to infinity, which results in singular problems.

To avoid the singularity problem of traditional TSM control, the NTSM switching function can be designed as

$$s = \dot{e} + \frac{1}{\alpha} \dot{e}^{p/q} \quad (8)$$

where $1 < p/q < 2$.

It can be proved that the control action obtained by the sliding mode surface designed by Equation (8) does not contain a negative exponential term, and the control quantity does not have an infinite term, thus solving the singularity problem of traditional TSM control.

However, if $s = 0$, the error convergence rate

$$\dot{e} = (-\alpha e)^{q/p}$$

and $0.5 < q/p < 1$. Therefore, when the system state is far away from the equilibrium point, the error convergence rate becomes slower.

In order to further improve the convergence speed of the NTSM switching function, the following NFTSM switching function is used

$$s = e + \dot{e}^{a_1} + \frac{1}{\alpha} \dot{e}^{a_2} \tag{9}$$

where a_1 and a_2 are design constants, and $1 < a_2 < 2, a_2 < a_1$.

Let $s = 0$, we have

$$\dot{e} = (-\alpha e - \alpha e^{a_1})^{1/a_2}$$

That is, when the system state is far away from the equilibrium point, the error convergence rate is mainly affected by the high-order term of e , and the convergence rate of NFTSM is faster than NTSM. When the system state is close to the equilibrium point, the convergence rate of NFTSM is similar to NTSM. Therefore, during the whole sliding stage, compared with NTSM, NFTSM control can achieve global fast convergence, and the exponential term in Equation (9) is greater than one, which eliminates the singularity problem of the control quantity.

Furthermore, in order to avoid the complex solution of the switching function of Equation (9) when $e < 0$ and $\dot{e} < 0$, the sliding mode switching function can be improved as

$$s = e + k_1 |e|^{a_1} \text{sgn}(e) + k_2 |\dot{e}|^{a_2} \text{sgn}(\dot{e}) \tag{10}$$

where $k_1 > 0$ and $k_2 > 0$ are design constants.

Taking the derivative of s and substituting it into Equation (5) yields

$$\begin{aligned} \dot{s} &= \dot{e} + k_1 a_1 |e|^{a_1-1} \dot{e} + k_2 a_2 |\dot{e}|^{a_2-1} \ddot{e} \\ &= \dot{e} + k_1 a_1 |e|^{a_1-1} \dot{e} + k_2 a_2 |\dot{e}|^{a_2-1} (\ddot{x}_2 - \ddot{x}_d) \\ &= \dot{e} + k_1 a_1 |e|^{a_1-1} \dot{e} + k_2 a_2 |\dot{e}|^{a_2-1} \left(\frac{k_T i_1 \eta_1}{J} u + \frac{1}{J} (T_G - T_R - T_f) + d - \ddot{x}_d \right) \end{aligned} \tag{11}$$

In order to further accelerate the convergence speed of the system and weaken the chattering, the exponential approximation law is used to design the controller. The expression is as follows

$$\dot{s} = k_2 a_2 |\dot{e}|^{a_2-1} (-ks - (U + \eta) \text{sgn}(s)) \tag{12}$$

where $k > 0$ is the exponential approach coefficient.

Combining Equations (11) and (12), the control law of the picking manipulator can be designed as

$$u = \frac{J}{k_T i_1 \eta_1} \left(-\frac{1}{k_2 a_2} |\dot{e}|^{2-a_2} \text{sgn}(\dot{e}) - \frac{k_1 a_1}{k_2 a_2} |e|^{a_1-1} |\dot{e}|^{2-a_2} \text{sgn}(\dot{e}) - ks - (U + \eta) \text{sgn}(s) - \frac{1}{J} (T_G - T_R - T_f) + \ddot{x}_d \right) \tag{13}$$

It can be seen that there is a positive term in Equation (13), and the control input will not produce an infinite quantity, which avoids the singular problem of traditional TSM. However, Equation (13) contains an unknown upper bound U of uncertainty, which makes it impossible to apply the control law directly. Therefore, an adaptive law is proposed in this paper to estimate the upper bound U of uncertainty, which is expressed as

$$\dot{\hat{U}} = \gamma k_2 a_2 |\dot{e}|^{a_2-1} |s| \tag{14}$$

where $\gamma > 0$ is adaptive gain.

To sum up, the adaptive nonsingular fast terminal sliding mode control law (ANFTSM) of the picking manipulator in this paper can be designed as

$$u = \frac{J}{k_T i_1 \eta_1} \left(-\frac{1}{k_2 a_2} |\dot{e}|^{2-a_2} \text{sgn}(\dot{e}) - \frac{k_1 a_1}{k_2 a_2} |e|^{a_1-1} |\dot{e}|^{2-a_2} \text{sgn}(\dot{e}) - ks - (\hat{U} + \eta) \text{sgn}(s) - \frac{1}{J} (T_G - T_R - T_f) + \ddot{x}_d \right) \quad (15)$$

3.2. Stability Analysis

The following lemma is used to prove the stability of the controller designed in this paper.

Lemma 1 [27]. For nonlinear system

$$\dot{x} = f(x, t), x \in \mathbb{R}^n \quad (16)$$

Suppose that there exists a continuously differentiable positive definite function $V(x)$ such that the following equation holds

$$\dot{V}(x) \leq -\mu V(x) - \lambda V^m(x) \quad (17)$$

where μ, λ , and m are positive numbers, and $0 < m < 1$. The initial state of the Equation (16) is denoted as $x_0 = x(t_0)$, and t_0 is the initial time of the Equation (16).

Then the system state converges to the equilibrium point in finite time. The convergence time is T , and

$$T \leq \frac{1}{\mu(1-m)} \ln \frac{\mu V^{1-m}(x_0) + \lambda}{\lambda}$$

Theorem 1. For the picking manipulator Equation (5), if the sliding mode switching function (10) and the approximation law (12) are selected, under the action of the adaptive law (14) and the control law (15) designed in this paper, the sliding mode switching function converges to zero in finite time, and the system position error e and speed error \dot{e} converge to zero in finite time.

Proof. The estimation error of the adaptive law is defined as $\tilde{U} = \hat{U} - U$, then $\dot{\tilde{U}} = \dot{\hat{U}}$.

Firstly, the estimation error of uncertainty is bounded is proved as follows.

Select the Lyapunov function

$$V_1 = \frac{1}{2} s^2 + \frac{1}{2\gamma} \tilde{U}^2 \quad (18)$$

Taking the derivative of V_1 and substitute into Equation (11) yields

$$\begin{aligned} \dot{V}_1 &= s\dot{s} + \frac{1}{\gamma} \tilde{U} \dot{\tilde{U}} \\ &= s(\dot{e} + k_1 a_1 |e|^{a_1-1} \dot{e} + k_2 a_2 |e|^{a_2-1} (\frac{k_T i_1 \eta_1}{J} u + \frac{1}{J} (T_G - T_R - T_f) + d - \ddot{x}_d)) + \frac{1}{\gamma} \tilde{U} \dot{\tilde{U}} \end{aligned} \quad (19)$$

Then, substitute Equation (19) into Equation (14) and Equation (15), and we can obtain

$$\begin{aligned} \dot{V}_1 &= s k_2 a_2 |\dot{e}|^{a_2-1} (-ks + d - (\hat{U} + \eta) \text{sgn}(s)) + \frac{1}{\gamma} \tilde{U} \gamma k_2 a_2 |\dot{e}|^{a_2-1} |s| \\ &= k_2 a_2 |\dot{e}|^{a_2-1} (-ks^2 + ds - (\hat{U} + \eta) |s| + (\hat{U} - U) |s|) \\ &\leq -k_2 a_2 |\dot{e}|^{a_2-1} (ks^2 + \eta |s|) \\ &\leq 0 \end{aligned} \quad (20)$$

It can be seen from the above Equation (20) that V_1 is bounded, so s and \tilde{U} are bounded, respectively. Then, let $|\tilde{U}| \leq \varepsilon$, ε is the upper bound of the estimation error \tilde{U} .

Furthermore, the following will prove that the sliding mode switching function can converge in finite time.

Reselect the Lyapunov function

$$V_2 = \frac{1}{2}s^2 \quad (21)$$

Taking the derivative of V_2 and substitute into Equation (11) yields

$$\begin{aligned} \dot{V}_2 &= s\dot{s} \\ &= \dot{e} + k_1 a_1 |e|^{a_1-1} \dot{e} + k_2 a_2 |e|^{a_2-1} \left(\frac{k_{r1} \eta_1}{J} u + \frac{1}{J} (T_G - T_R - T_f) + d - \ddot{x}_d \right) \end{aligned} \quad (22)$$

Substitute Equation (22) into Equations (14) and (15), we have

$$\begin{aligned} \dot{V}_2 &= s k_2 a_2 |\dot{e}|^{a_2-1} (-ks + d - (\hat{U} + \eta) \operatorname{sgn}(s)) \\ &\leq k_2 a_2 |\dot{e}|^{a_2-1} (-ks^2 + U|s| - (\hat{U} + \eta)|s|) \\ &= k_2 a_2 |\dot{e}|^{a_2-1} (-ks^2 - \tilde{U}|s| - \eta|s|) \\ &\leq k_2 a_2 |\dot{e}|^{a_2-1} (-ks^2 + (\varepsilon - \eta)|s|) \\ &= -k_2 a_2 |\dot{e}|^{a_2-1} (ks^2 + (\eta - \varepsilon)|s|) \\ &= -\lambda_1 V_2 - \lambda_2 V_2^{1/2} \end{aligned} \quad (23)$$

where

$$\begin{aligned} \lambda_1 &= 2k k_2 a_2 |\dot{e}|^{a_2-1} \\ \lambda_2 &= \sqrt{2}(\eta - \varepsilon) k_2 a_2 |\dot{e}|^{a_2-1} \end{aligned}$$

When $\dot{e} \neq 0$, there is $|\dot{e}|^{a_2-1} > 0$, by selecting parameter $\eta > \varepsilon$, we can obtain

$$\lambda_1 > 0, \lambda_2 > 0, \dot{V}_2 \leq -\lambda_1 V_2 - \lambda_2 V_2^{1/2}$$

By Lemma 1, it can be seen that the system will converge to $s = 0$ in finite time, and the convergence time satisfies

$$t_r \leq \frac{2}{\lambda_1} \ln \frac{\lambda_1 V_2^{1/2}(x_0) + \lambda_2}{\lambda_2}$$

where $V_2(x_0)$ is the initial value of $V_2(x)$.

When $\dot{e} = 0$, during the system state sliding to the system equilibrium point stage, there is $s \neq 0$. Substitute Equation (15) into Equation (5), we can obtain

$$\ddot{e} = -ks + d - (\hat{U} + \eta) \operatorname{sgn}(s) \neq 0$$

which derives a contradiction. This means that the system state will not remain at this point, and the system state will converge to $s = 0$ in finite time.

When the system state reaches the sliding surface $s = 0$, it can be known from Equation (10) that the system state is determined by the following nonlinear equation

$$e + k_1 |e|^{a_1} \operatorname{sgn}(e) + k_2 |\dot{e}|^{a_2} \operatorname{sgn}(\dot{e}) = 0 \quad (24)$$

According to [28], e and \dot{e} converge to zero in finite time. The convergence time t_s is

$$t_s = \frac{a_2 |e(t_r)|^{1-1/a_2}}{k_1 (a_2 - 1)} \cdot F\left(\frac{1}{a_2}, \frac{a_2 - 1}{(a_1 - 1)a_2}; 1 + \frac{a_2 - 1}{(a_1 - 1)a_2}; -k_1 |e(t_r)|^{a_1-1}\right)$$

where $F(\cdot)$ is a Gaussian hypergeometric function. \square

3.3. Friction Parameter Identification

Nonlinear friction appears in large quantities in electromechanical servo systems. Its nonlinear time-varying characteristic is one of the important factors affecting the control effect of the system. In order to improve the control performance, effective compensation strategies should be adopted to reduce the influence of friction on the system.

In this paper, the Stribeck friction model is used to identify the friction force during the movement of the picking manipulator. The Stribeck friction model expression can be written as

$$T_f = \begin{cases} F_c^+ + (F_s^+ - F_c^+)e^{-\left(\frac{\dot{\theta}}{v_s^+}\right)^2} \text{sgn}(\dot{\theta}) + \sigma^+\dot{\theta}, & \dot{\theta} > 0 \\ F_c^- + (F_s^- - F_c^-)e^{-\left(\frac{\dot{\theta}}{v_s^-}\right)^2} \text{sgn}(\dot{\theta}) + \sigma^-\dot{\theta}, & \dot{\theta} < 0 \end{cases} \quad (25)$$

where F_c and F_s are Coulomb friction torque and maximum static friction torque, respectively. v_s is the Stribeck speed, σ is the viscous friction coefficient.

In this paper, the genetic algorithm [24] is used to identify these parameters such as F_c^+ , F_c^- , F_s^+ , F_s^- , F_c^+ , F_c^- , v_s and σ in (25). The specific identification process is as follows.

Firstly, disconnect the connection between the picking manipulator and the equilibrator, and the system dynamics equation is transformed into

$$J\ddot{\theta} = i_1\eta_1k_T I - T_f \quad (26)$$

where I is the control current of the system. Let the motor move with a set of constant speed $(\dot{\theta})_{i=1}^N$ and record the average current value $(I)_{i=1}^N$ at different speeds.

It can be seen from Equation (26) that if $\ddot{\theta} = 0$, then we have $T_f = i_1\eta_1k_T I$, such that the relationship between current and speed is determined by the sequence $(I)_{i=1}^N$ and $(\dot{\theta})_{i=1}^N$.

Let the identification vector be

$$x_s = [F_c^+ \quad F_s^+ \quad v_s^+ \quad \sigma^+ \quad F_c^- \quad F_s^- \quad v_s^- \quad \sigma^-] \quad (27)$$

and denote the identification error as

$$e_I(x_s, \dot{\theta}) = i_1\eta_1k_T I - T_f(x_s, \dot{\theta}) \quad (28)$$

Take the objective function as

$$J_e = \frac{1}{2} \sum_{i=1}^N e_I^2(x_s, \dot{\theta}) \quad (29)$$

Then, the problem of solving the friction parameter in (27) is transformed into solving the minimum value problem of the objective function J_e . The parameter identification process using the genetic algorithm is as follows.

Step 1. Initializing the population $P(0)$ randomly, and $X_i(i = 1, 2, \dots, M)$ is the individual in the population, t is the evolution algebra, let the maximum evolution algebra is $T = 10,000$, the population size is $M = 300$.

Step 2. Calculating the Individual Fitness Function

$$f(X_i) = \frac{1}{J_e(X_i)} \quad (30)$$

Step 3. Determine whether t is equal to T , if $t = T$, output the results of the identification parameters, otherwise turn to the next step.

Step 4. Saving the random sampling of the best individual for selection operation, and forming the next generation population $P(t)$.

- Step 5. Perform the crossover operation with the uniform crossover operator $p_c = 0.9$.
- Step 6. Set the adaptive mutation operator $p_m = 0.1 - 0.099t/T$ for mutation operation.
- Step 7. Set $t = t + 1$, repeat step (2)–(6), and output the final optimal solution, which is the identification result.

4. Simulation

In this section, a simulation example of a single joint picking manipulator is provided to illustrate the theoretical result. In order to simplify the experimental device, the gas spring is used instead of the balancer. The parameter of Equation (5) is shown in Table 1.

Table 1. Parameters of the picking manipulator.

Parameters	Value
p_0	0.35/MPa
S	$6.8 \times 10^{-5}/m^2$
V_0	$7.654 \times 10^{-5}/m^3$
n	1.2
i_1	630
α_1, α_2	0

The structure diagram of the control system is shown in Figure 2.

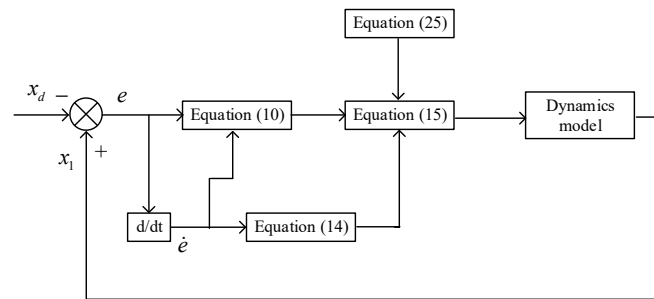


Figure 2. The structure diagram of the control system.

Firstly, in order to realize the compensation control of friction, the genetic algorithm in Section 3 is used to identify the friction parameters of the picking manipulator prototype. The comparison of experimental results and identification results is shown in Figure 3, and the identification results of model parameters are shown in Table 2. It can be seen from Figure 3 that the identification curve is consistent with the experimental curve, indicating that the identified parameters are accurate and reasonable. The identification results can be substituted into the control law for compensation design.

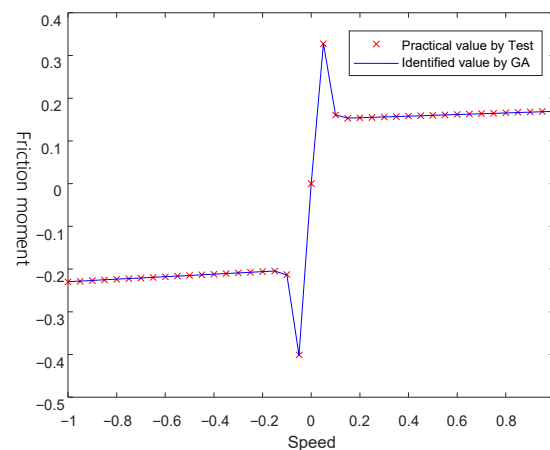


Figure 3. Friction parameter identification curve.

Table 2. Friction parameter identification results.

Parameters	Identification Results
F_c^+	7.2401/Nm
F_s^+	6.0127/Nm
F_c^-	0.3102/Nm
F_s^-	6.2149/Nm
v_s^+	0.3660 rad/s
v_s^-	1.2681 rad/s
σ^+	0.9460 Nms/rad
σ^-	1.7982 Nms/rad

In order to suppress the chattering problem in sliding mode control effectively, the saturation function $sat(s)$ is used instead of $sgn(s)$.

$$sat(s) = \begin{cases} 1, & s > \Delta \\ s/\Delta, & |s| \leq \Delta \\ -1, & s < -\Delta \end{cases}$$

where $\Delta = 0.05$ is the boundary layer thickness constant.

Other control parameters in this paper are selected as $k_T = 35 \text{ mN}\cdot\text{m}/\text{A}$, $\eta_1 = 0.9$, $a_1 = 2$, $a_2 = 1.5$, $k_1 = 200$, $k_2 = 10$, and $\eta = 0.1$.

In this section, two different simulations are carried out, and the load of the picking manipulator is set to 0.5 kg and 1.5 kg, respectively. The control objective is to control the picking manipulator to track the desired trajectory $x_d = 0.1 \sin(t)$, and the initial state of the system is $x(0) = 0, \dot{x}(0) = 0$.

In the first case, when the load of the manipulator is 0.5 kg, the simulation results are shown in Figures 4–6.

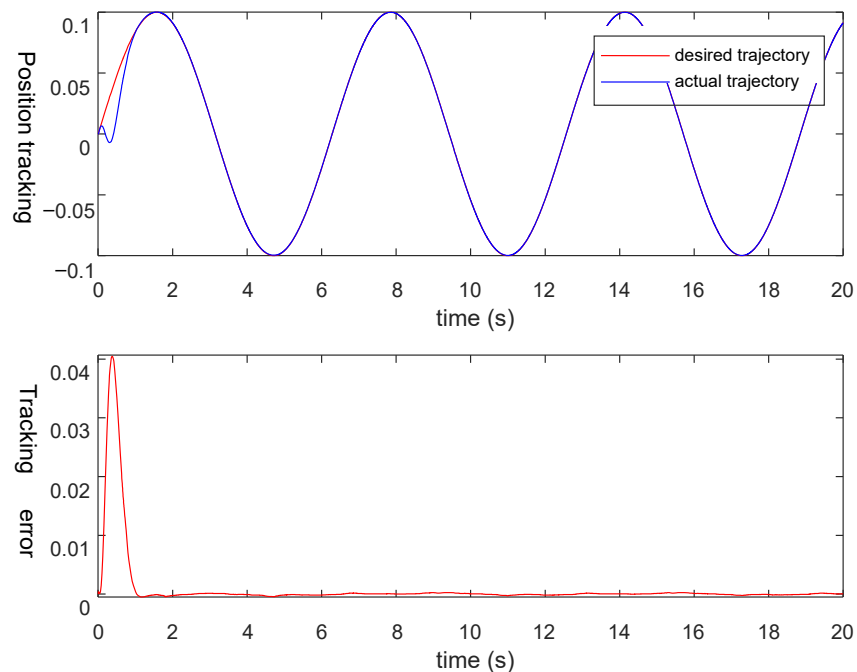


Figure 4. Position tracking curve and tracking error curve.

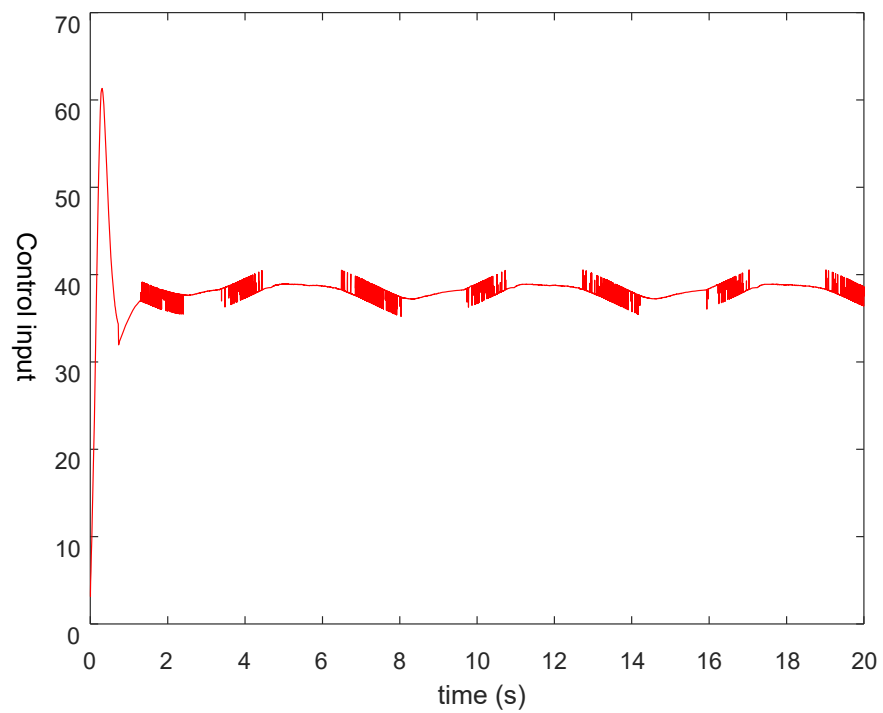


Figure 5. The control input of the system.

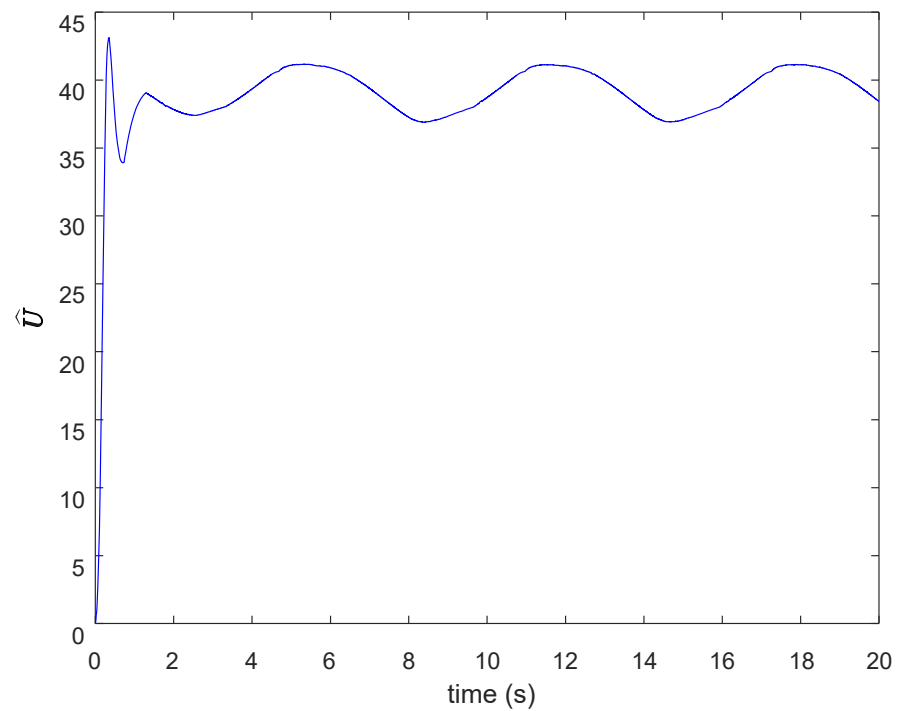


Figure 6. Estimation of the upper bound of uncertainty.

In the second case, when the load of the manipulator is 1.5 kg, the simulation results are shown in Figures 7–9.

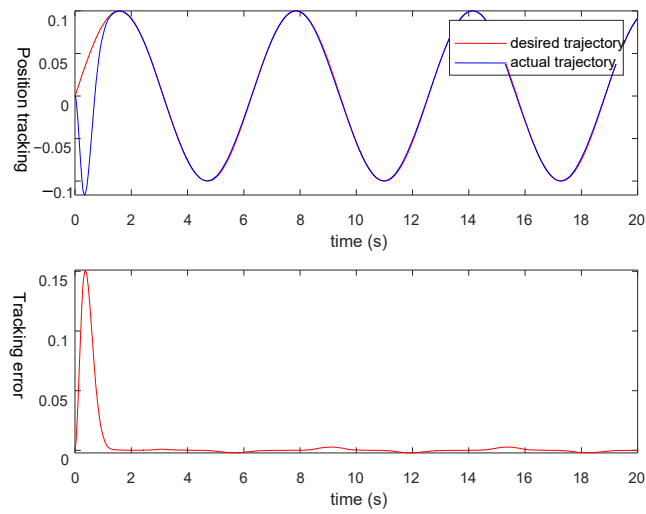


Figure 7. Position tracking curve and tracking error curve.

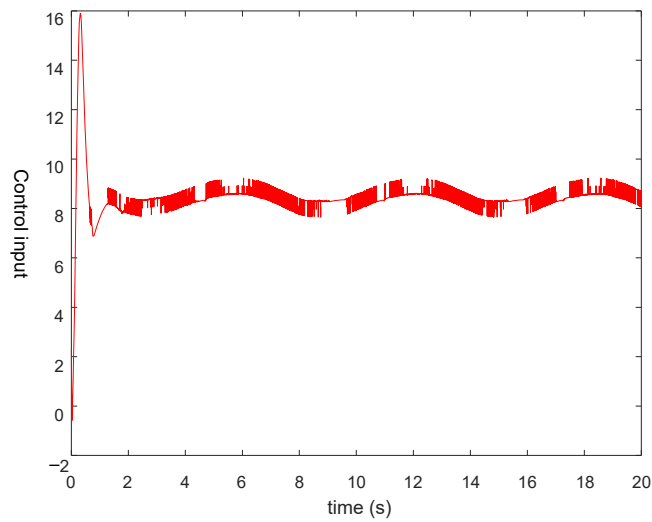


Figure 8. The control input of the system.

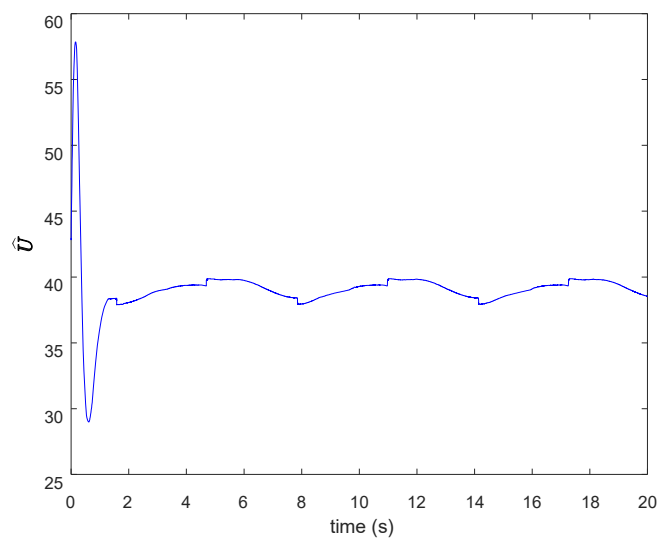


Figure 9. Estimation of the upper bound of uncertainty.

It can be seen from Figures 4 and 7 that the joint trajectory can track the desired trajectory at 1.101 s and 1.502 s, respectively. The tracking error can also converge to the equilibrium position rapidly under the controller designed in this paper. It shows that the ANFTSM control algorithm designed in this paper has strong robustness to load parameter changes and nonlinear friction. It also can be seen from Figures 5 and 8 that the control input does not produce singular problems under different loads. Figures 6 and 9 show the convergence of the adaptive estimation of the uncertainty, which avoids the problem of control chattering caused by taking a too large uncertainty upper bound in the absence of uncertainty prior knowledge, and is more conducive to practical engineering applications.

In order to assess the control strategy synthesized in this paper, a comparative analysis is established to examine the performance of the ANFTSM control algorithm across the traditional sliding mode control scheme. The load of the manipulator is set as 1 kg. The simulation results are depicted in Figures 10 and 11, which represent the system's trajectory tracking curves and the resultant control inputs, respectively.

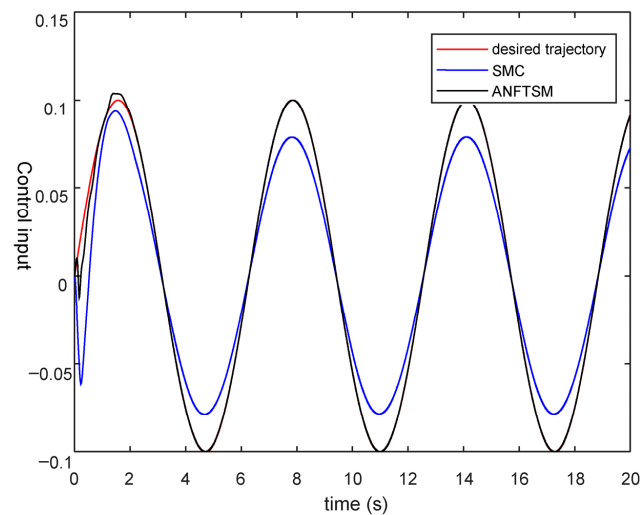


Figure 10. Position tracking curve.

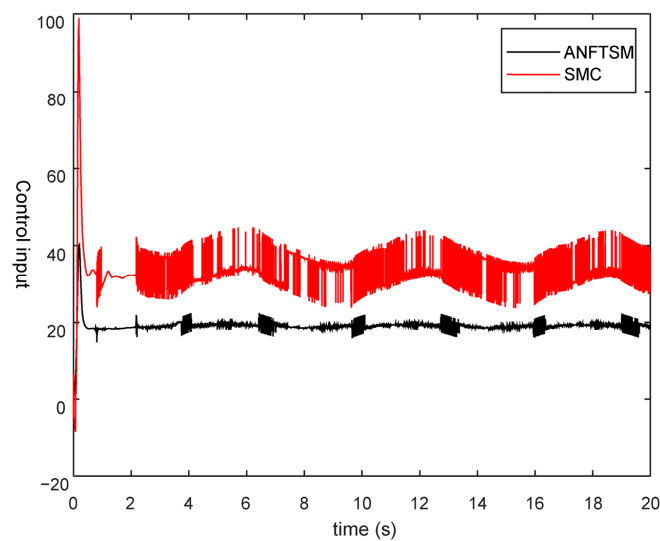


Figure 11. Control input.

It can be seen from Figures 10 and 11 that compared with the traditional sliding mode control method, the proposed method in this paper has great advantages in tracking accuracy and convergence time.

5. Conclusions

In this paper, the dynamic model of the picking manipulator is analyzed, and a new NFTSM control algorithm is used to design the corresponding position controller, which avoids the singularity problem of the traditional terminal sliding mode control and the slow convergence of the traditional NTSM control. At the same time, the adaptive estimation of the system uncertainty is used without the prior knowledge of the upper bound of the uncertainty, which effectively reduces the chattering caused by the excessive switching gain. Aiming at the nonlinear friction disturbance in the motion process of the picking manipulator system, the genetic algorithm is used to identify the friction parameters, and the obtained parameters are used for the compensation control of the picking manipulator. The simulation results show that the controller can achieve fast and accurate positioning of the picking manipulator under different load conditions. The designed controller has good robustness and is easy to apply in engineering practice.

Future development work will focus on applying new algorithms to approximate system uncertainties, such as meta heuristic algorithms. In addition, how to use the optimization algorithm to obtain the optimal adjustment parameters of the controller can be considered.

Author Contributions: Conceptualization, C.W. and S.Z.; methodology, C.W.; software, S.Z.; validation, C.W. and S.Z.; formal analysis, C.W. and S.Z.; investigation, S.Z.; resources, S.Z.; data curation, C.W. and S.Z.; writing—original draft preparation, S.Z.; writing—review and editing, C.W. and S.Z.; visualization, C.W. and S.Z.; supervision, C.W. and S.Z.; project administration, C.W. and S.Z.; funding acquisition, C.W. All authors have read and agreed to the published version of the manuscript.

Funding: This research was funded by National Natural Science Foundation of China, grant number 61078070; the open project of Key Laboratory of Grain Information Processing and Control, grant number KFJJ-2021-110.

Institutional Review Board Statement: Not applicable.

Informed Consent Statement: Not applicable.

Data Availability Statement: Not applicable.

Conflicts of Interest: The authors declare no conflict of interest. The funders had no role in the design of the study; in the collection, analyses, or interpretation of data; in the writing of the manuscript, or in the decision to publish the results.

References

1. Wang, J.; Cheng, Z.; Zhang, F. Design of the Divided No-till Wheat Planter Orchard Picking Manipulator Research. *J. Agric. Mech. Res.* **2020**, *14*, 158–163.
2. Yu, X.; Fan, Z.; Wang, X.; Wan, H.; Wang, P.; Zeng, X.; Jia, F. A lab-customized autonomous humanoid apple harvesting robot. *Comput. Electr. Eng.* **2021**, *96*, 107459. [[CrossRef](#)]
3. Fang, Z.; Liang, X.F. Intelligent obstacle avoidance path planning method for picking manipulator combined with artificial potential field method. *Ind. Robot* **2022**, *49*, 835–850. [[CrossRef](#)]
4. Schuetz, C.; Baur, J.; Pfaff, J.; Buschmann, T.; Ulbrich, H. Evaluation of a direct optimization method for trajectory planning of a 9-DOF redundant fruit-picking manipulator. In Proceedings of the 2015 IEEE International Conference on Robotics and Automation (ICRA), Seattle, WA, USA, 26–30 May 2015; pp. 2660–2666.
5. Liu, Y.C.; Yan, W.; Zhang, T.; Yu, C.X.; Tu, H.Y. Trajectory Tracking for a Dual-Arm Free-Floating Space Robot with a Class of General Nonsingular Predefined-Time Terminal Sliding Mode. *IEEE Trans. Syst. Man Cybern. Syst.* **2022**, *52*, 3273–3286. [[CrossRef](#)]
6. Khurram, A.; Adeel, M.; Jamshed, I. Terminal Sliding Mode Control of an Anthropomorphic Manipulator with Friction Based Observer. In Proceedings of the 2021 International Conference on Robotics and Automation in Industry, Xi'an, China, 30 May–5 June 2021; pp. 143–150.
7. Xu, H.; Li, M.; Lu, C.L. Nonlinear sliding mode control of manipulator based on iterative learning algorithm. *J. Electr. Syst.* **2021**, *17*, 421–437.
8. Su, L.Q.; Guo, X.; Ji, Y. Tracking control of cable-driven manipulator with adaptive fractional-order nonsingular fast terminal sliding mode control. *JVC/J. Vib. Control* **2021**, *27*, 2482–2493. [[CrossRef](#)]
9. Lu, Z.P.; Li, Y.; Fan, X.; Li, Y.C. Decentralized Fault Tolerant Control for Modular Robot Manipulators via Integral Terminal Sliding Mode and Disturbance Observer. *Int. J. Control Autom. Syst.* **2022**, *20*, 3274–3284. [[CrossRef](#)]

10. Zaare, S.; Soltanpour, M.R. Adaptive fuzzy global coupled nonsingular fast terminal sliding mode control of n-rigid-link elastic-joint robot manipulators in presence of uncertainties. *Mech. Syst. Signal Process.* **2022**, *163*, 108165. [[CrossRef](#)]
11. Song, T.Z.; Fang, L.; Wang, H.Z. Model-free finite-time terminal sliding mode control with a novel adaptive sliding mode observer of uncertain robot systems. *Asian J. Control* **2022**, *24*, 1437–1451. [[CrossRef](#)]
12. Boukattaya, M.; Mezghani, N.; Damak, T. Adaptive nonsingular fast terminal sliding-mode control for the tracking problem of uncertain dynamical systems. *ISA Trans.* **2018**, *77*, 1–19. [[CrossRef](#)]
13. Zhang, S.J.; Cao, Y. Cooperative Localization Approach for Multi-Robot Systems Based on State Estimation Error Compensation. *Sensors* **2019**, *19*, 3842–3852. [[CrossRef](#)] [[PubMed](#)]
14. Wang, Y.; Li, B.; Yan, F. Practical adaptive fractional-order nonsingular terminal sliding mode control for a cable-driven manipulator. *Int. J. Robust Nonlinear Control* **2019**, *29*, 1396–1417. [[CrossRef](#)]
15. Hao, S.; Hu, L.Y.; Liu, P. Second-order adaptive integral terminal sliding mode approach to tracking control of robotic manipulators. *IET Control Theory Appl.* **2021**, *15*, 2145–2157. [[CrossRef](#)]
16. Van, M.; Mavrovouniotis, M.; Ge, S.Z. An adaptive backstepping nonsingular fast terminal sliding mode control for robust fault tolerant control of robot manipulators. *IEEE Trans. Syst. Man Cybern. Syst.* **2019**, *49*, 1448–1458. [[CrossRef](#)]
17. Shao, X.Y.; Sun, G.H.; Xue, C. Nonsingular terminal sliding mode control for free-floating space manipulator with disturbance. *Acta Astronaut.* **2021**, *181*, 396–404. [[CrossRef](#)]
18. Zhang, S.; Cao, Y. Consensus in networked multi-robot systems via local state feedback robust control. *Int. J. Adv. Robot. Syst.* **2019**, *16*, 1–7. [[CrossRef](#)]
19. Wang, Y.M.; Han, F.L.; Feng, Y. Hybrid continuous nonsingular terminal sliding mode control of uncertain flexible manipulators. In Proceedings of the IECON Proceedings (Industrial Electronics Conference), Dallas, TX, USA, 29 October–1 November 2014; pp. 190–196.
20. Fang, H.R.; Wu, Y.; Xu, T.; Wan, F.X. Adaptive neural sliding mode control of uncertain robotic manipulators with predefined time convergence. *Int. J. Robust Nonlinear Control* **2022**, *32*, 223–238. [[CrossRef](#)]
21. Mourad, K.; Magdi, S.M. Robust-QSR γ -dissipative sliding mode control for uncertain discrete-time descriptor systems with time-varying delay. *IMA J. Math. Control Inf.* **2018**, *35*, 735–756.
22. Charfeddine, S.; Boudjemline, A.; Ben Aoun, S.; Jerbi, H.; Kchaou, M.; Alshammari, O.; Elleuch, Z.; Abbassi, R. Design of a fuzzy optimization control structure for nonlinear systems: A disturbance-rejection method. *Appl. Sci.* **2021**, *11*, 2612. [[CrossRef](#)]
23. Abbassi, A.; Ben Mehrez, R.; Bensalem, Y.; Abbassi, R.; Kchaou, M.; Jemli, M.; Abualigah, L.; Altalhi, M. Improved Arithmetic Optimization Algorithm for Parameters Extraction of Photovoltaic Solar Cell Single-Diode Model. *Arab. J. Sci. Eng.* **2022**, *47*, 10435–10451. [[CrossRef](#)]
24. Yang, G.C.; Yao, J.Y.; Dong, Z.L. Neuroadaptive learning algorithm for constrained nonlinear systems with disturbance rejection. *Int. J. Robust Nonlinear Control* **2022**, *32*, 6127–6147. [[CrossRef](#)]
25. Yang, G.C.; Yao, J.Y.; Dong, Z.L. Multilayer neuroadaptive force control of electro-hydraulic load simulators with uncertainty rejection. *Appl. Soft Comput.* **2022**, *130*, 109672. [[CrossRef](#)]
26. Zhou, X.; Zhao, B.; Liu, W. A compound scheme on parameters identification and adaptive compensation of nonlinear friction disturbance for the aerial inertially stabilized platform. *ISA Trans.* **2017**, *67*, 293–305. [[CrossRef](#)] [[PubMed](#)]
27. Si, Y.J.; Song, S.M. Adaptive reaching law based three-dimensional finite-time guidance law against maneuvering targets with input saturation. *Aerosp. Sci. Technol.* **2017**, *70*, 198–210. [[CrossRef](#)]
28. Sun, H.Q.; Zhang, S.J.; Quan, Q.L. Trajectory Tracking Robust Control Method Based on Finite-Time Convergence of Manipulator with Nonsingular Fast Terminal Sliding Mode Surface. *J. Control Sci. Eng.* **2022**, *2022*, 2271804. [[CrossRef](#)]